Harmonic Analysis in Grease Rheology

Thomas E. Karis,[1] Raymond-Noël Kono,[2,3] Myung S. Jhon[2]

[1]*Hitachi Global Storage Technologies, San Jose Research Center, San Jose, CA 95120-6099*
[2]*Department of Chemical Engineering, Carnegie Mellon University, Pittsburgh, PA 15213-3890*
[3]*Intel Corporation, Optical Platform Division, Newark, CA 94560*

Received 17 May 2002; accepted 31 December 2002

ABSTRACT: Yield stress, and small- and large- amplitude oscillatory shear measurements were performed on greases in a cone-plate fixture. Below the yield point, the grease behavior mimics that of a lightly crosslinked polymer. In large-amplitude oscillations that exceed the yield stress, harmonic distortion appears in the stress waveform. The elastic component of the stress is continuous across the transition, while the viscous, or out-of-phase component, is a transient stress that occurs in the high shear rate portion of each oscillation cycle. Our newly proposed viscous slip model accurately reproduces the measured stress waveform for greases, as well as for other yield stress materials. From measured harmonic amplitudes, this model provides the strain amplitude dependence of the elastic modulus and the equivalent of a dynamic yield stress. These properties of channeling grease complement the conventional measurements of yield stress and worked and unworked penetration. © 2003 Wiley Periodicals, Inc. J Appl Polym Sci 90: 334–343, 2003

INTRODUCTION

Lubricating greases are composed of a gelling agent and lubricating oil. Therefore, greases possess polymer network-like characteristics that determine the rheological properties of the lubricating grease.[1] As this work pertains to industrial applications, the yield stress is essential for holding a channeling grease in place within a ball bearing. Greases present a challenge to bearing design with finite element modeling because of their complicated flow properties. Criddle[2] reported that grease properties depend on shear history. Shearing greases above the yield stress, σ_y, produces non-Newtonian behavior. Stress relaxation of greases is also non-Newtonian. Evans et al.[3] studied the mechanical behavior of sodium and lithium greases near the yield point. They suggested that lithium grease contains a dispersion of soap fibers in oil, where the fibers form aggregates which in turn are capable of linking up through the operation of weak attractive forces. A modified Kelvin element was employed to examine the viscoelastic properties of the materials; the superposition principle did not apply, and the power law failed to describe shear-thinning behavior adequately. Binding et al.[4] reported difficulties in measuring the normal stress of lubrication greases with a Weissenberg rheometer, due to shear induced degradation and wall effects caused by fracture and yield stress. Mas and Magnin[1] studied the rheology of lithium and sodium greases. They reported that lithium greases displayed a yield stress, and that sodium greases had a minimum in the shear stress versus shear rate curve.

Grease flow behavior is complicated by time-dependent viscoelastic properties arising from the breakdown and reformation of microstructures. Dynamic mechanical measurements are typically used to study the structures of complex emulsions, dispersions, gels and slurries that may exhibit yield stress.[5] Above the yield stress or strain, the material exhibits viscous flow behavior. The existence and determination of yield stress continues to be a widely debated topic: Wardhaugh and Boger[6] studied the yield stress of waxes using cone-plate geometry and vane tests. Their results emphasized the complexity of the three distinct material states accompanying the yield behavior of waxy oil. These non-Newtonian flow characteristics are attributed to the interactions of particle clusters that have finite cohesive strengths.

In the past, the material properties were typically characterized via small amplitude oscillatory shear, with linear viscoelastic storage and loss shear moduli.[7,8] More recently, we performed Large Amplitude Oscillatory Shear (LAOS) measurements to examine the rheological properties of thixotropic polymer melts and particle suspensions.[9,10] However, the stress response in LAOS is too complex for characterization by linear viscoelasticity theory.[11–13] LAOS deforms the sample into the nonlinear conformation, resulting in harmonic distortion of the shear stress response. This interesting phenomenon has sparked investigations revealing the presence of harmonics in the LAOS re-

Correspondence to: T. Karis (email: Tom.Karis@hgst.com).

Journal of Applied Polymer Science, Vol. 90, 334–343 (2003)

sponse for a variety of rheologically complex materials. Yoshimura and Prud'homme[14] examined the effects of wall slip in oscillatory shear measurements. They attributed slip to the generation of large velocity gradients in a thin region adjacent to the wall, and adopted a Voigt-Kelvin constitutive equation to analyze its viscous and elastic effects. They found that LAOS flows of polymer melts between two parallel plates exhibit either quasi-periodic, nonperiodic, or chaotic responses. Reimers and Dealy[15] studied the dynamic nature of wall slip via LAOS. They found odd harmonics in the nonlinear response of a high molecular weight polystyrene solution. Wardhaugh and Boger[6] observed sinusoidal responses below the yield stress, but noted that distortions occur above the yield stress. They derived a yield stress from the in-phase component.

More recently, Wihelm et al.[16] examined the nonlinear response of a polyisobutylene solution via harmonic analysis. Increases in the higher harmonic contributions with the applied shear strain amplitude are described by an exponential function. They found that the odd harmonics become dominant at high shear strain amplitude.

Small amplitude oscillations provide the linear viscoelastic properties below the yield stress. LAOS yields Fourier components that are related to nonlinear properties of the material. In this study, a novel technique based on the discrete amplitude spectrum in LAOS was developed to examine thixotropic suspension rheology.

Greases exhibit solid-like behavior below the yield stress, and thixotropic behavior above the yield stress. The solid-like property is provided by a network structure of soap micelles in the case of lithium grease, or by a concentration above the percolation threshold in the case of particle thickened greases. For the ultimate modeling of grease flow in bearings, it is necessary to account for the entire range of grease behavior, including the dynamics of the yield structure breakdown and regeneration. Characterizations of the grease linear viscoelastic properties at small strain amplitude below the yield stress and measurement of the static yield stress are relatively straightforward. The present challenge is to quantify the dynamic nature of the yield transition and flow as the grease encounters cyclic stresses within the interstitial region between the balls, retainer, inner and outer race, and the bearing shields. This challenge is addressed by an analysis of grease flow in a well-defined LAOS flow. The presence of yield stress in the material gives rise to harmonic distortion in the waveform. Therefore, the goal for our initial study is to develop a feasible model of grease flow behavior that is consistent with LAOS waveforms and their spectral composition.

EXPERIMENTAL

Materials

One grease was a commercial fluorotelomer thickened perfluoropolyether (PFPE) grease with base oil and fluorotelomer thickener in a 3 to 1 ratio, and 1% rust inhibitor. The base oil was a K-type PFPE.[17] The number average molecular weight of the base oil was 6,600 Daltons from nuclear magnetic resonance spectroscopy, and the base oil viscosity was about 1.67 Pa s at 20°C.

Another type of grease examined was lithium grease with synthetic ester base oil and lithium 12-hydroxysterate thickener in a 9 to 1 ratio and additional antioxidants and antiwear additives.

A polyurea thickened grease with a paraffin base oil to thickener ratio of 6 to 1 and antirust and antiwear additives was also included in the yield stress-temperature measurements.

Apparatus

Controlled strain measurements were performed with a Rheometrics RMS 705 Mechanical Spectrometer and a 2,000 g cm torque transducer at 20°C. The cone-plate fixture was 50 mm in diameter with a 0.035 radian cone angle and a 50 micron gap. LAOS was applied to the greases with an increasing strain amplitude. An Analogic Data Precision Data 6000 waveform analyzer was used to calculate the magnitude spectrum from the stress transducer output voltage, and the spectrum was transferred to a personal computer.

Controlled stress measurements were performed with a Carrimed (now TA Instruments) CSL 500 stress rheometer. The cone-plate fixture was 40 mm in diameter, with a 0.035 radian cone angle and a 64 micron gap. The yield stress was measured by gradually increasing the stress level at a rate of 2 to 5 Pa s^{-1} until there was detectable angular displacement of the fixture. The yield stress measurement was completed when the shear rate reached 10^{-2} s^{-1} to minimize changes to the sample.

RESULTS AND DISCUSSION

Elastic region

The predominantly elastic behavior of grease below the yield stress is illustrated in Figure 1. The linear viscoelastic storage modulus G', and the loss modulus G'', change relatively little over a wide range of frequency (ω), and $G' \gg G''$. No terminal region was observed, and the response shown in Figure 1 is typical for all greases examined. Also, the linear viscoelastic properties were practically independent of temperature between 20 and 100°C.

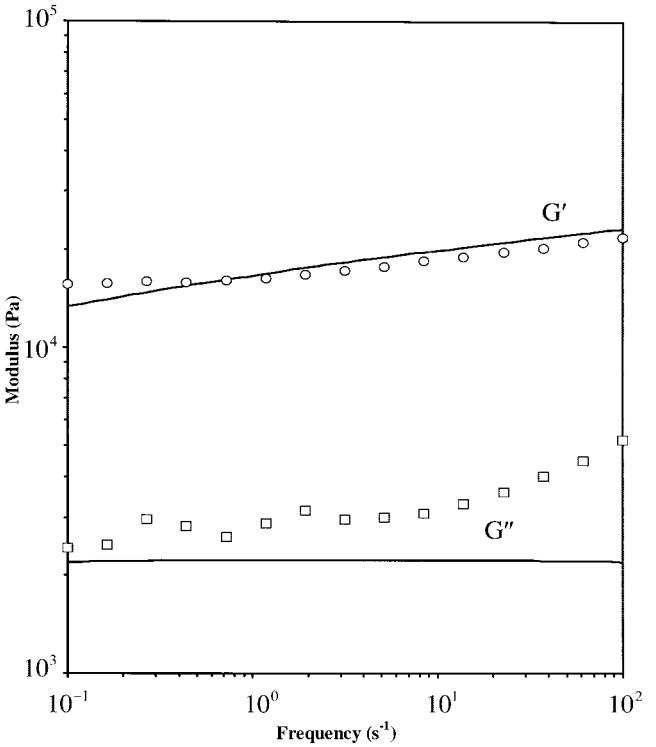

Figure 1 Storage and loss moduli as a function of frequency below the yield point for fluorotelomer grease. The equilibrium modulus G_e = 8 kPa and the relaxation spectrum H = 1.42 kPa at a strain amplitude of 0.005 and 20°C.

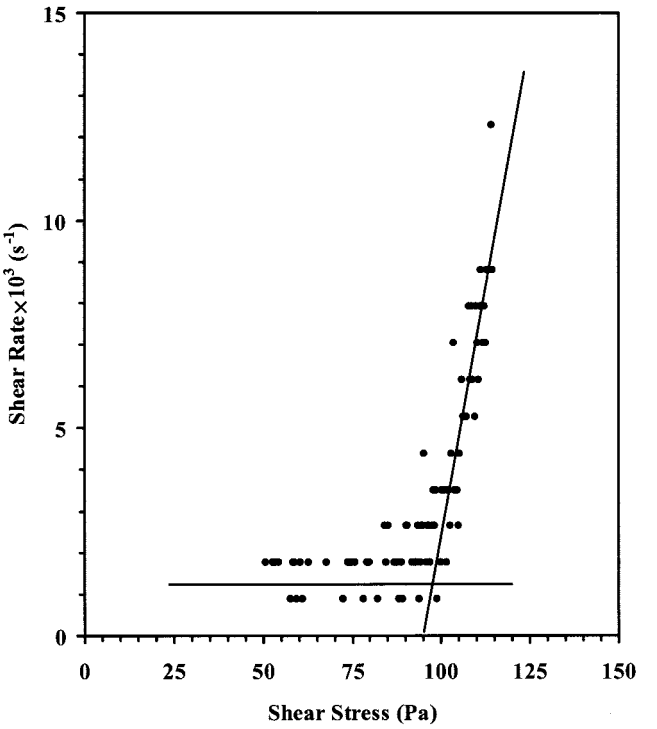

Figure 3 Shear rate as the shear stress is gradually increased in the conventional yield stress measurement on lithium grease in the stress rheometer. The lithium grease in this test was diluted by 36% with low viscosity oil.

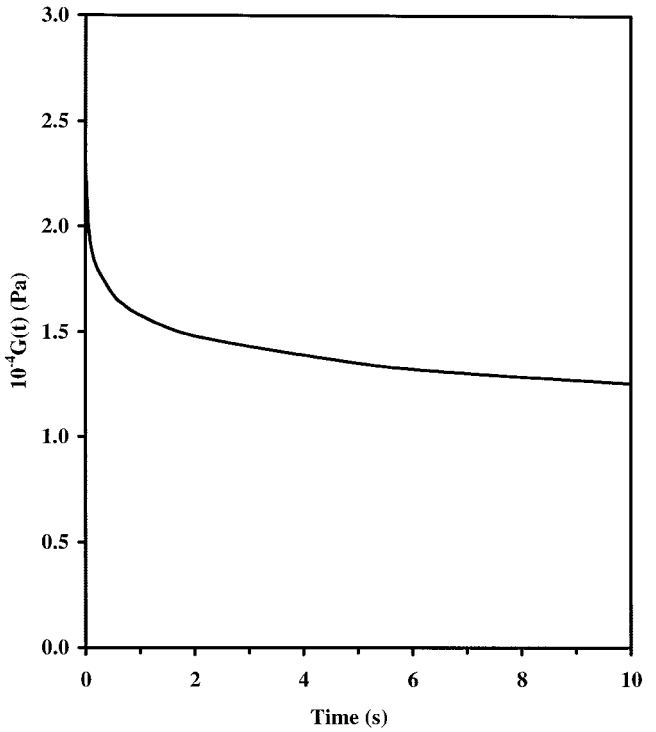

Figure 2 Shear modulus G(t) calculated from the G′ and G″ data in the elastic region below the yield stress for the fluorotelomer grease shown in Figure 1.

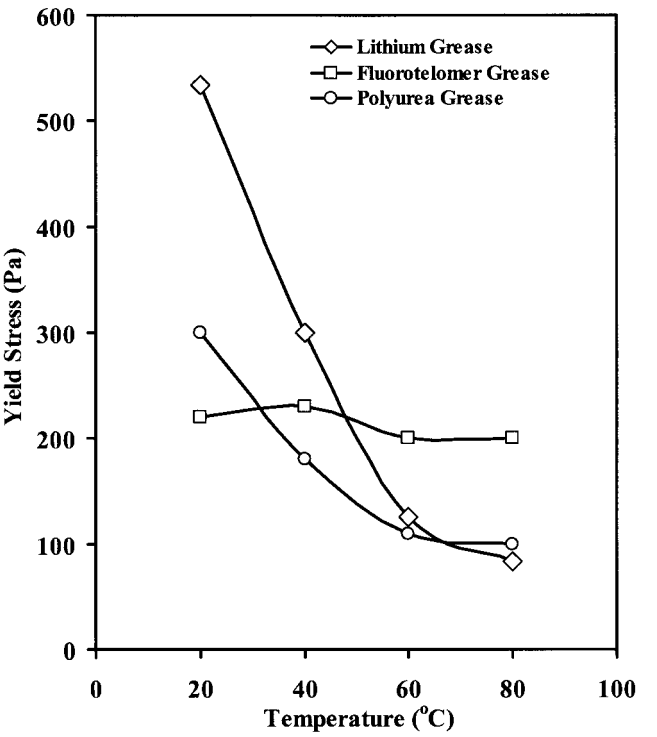

Figure 4 Yield stress measured (as in Figure 3) at different temperatures for the three different types of grease.

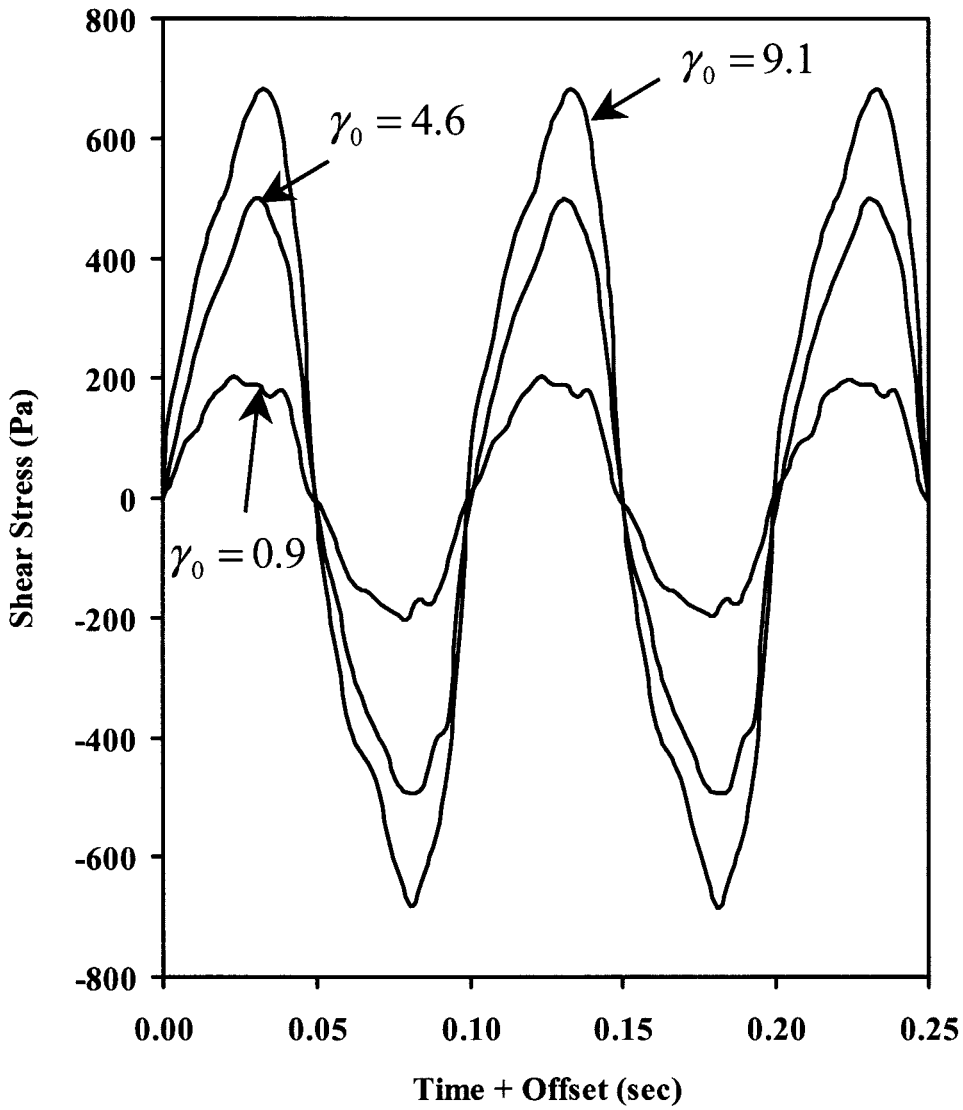

Figure 5 Typical shear stress waves at a frequency of 10 Hz for the fluorotelomer grease.

Linear viscoelastic properties can be expressed in terms of a relaxation time distribution. For greases, the response in the elastic region dictates a continuous relaxation time distribution, $H(\tau)$, where H is the magnitude of the relaxation at time τ such that G′, G″, shear modulus G(t), and shear viscosity η are expressed in terms of $H(\tau)$;

$$G' = G_e + \int_{-\infty}^{\infty} \frac{H(\omega\tau)^2}{1 + (\omega\tau)^2}\, dln\tau, \tag{1}$$

$$G'' = \int_{-\infty}^{\infty} \frac{H\omega\tau}{1 + (\omega\tau)^2}\, dln\tau, \tag{2}$$

$$G(t) = G_e + \int_{-\infty}^{\infty} He^{-t/\tau} dln\tau, \tag{3}$$

and

$$\eta = \int_{-\infty}^{\infty} H\tau dln\tau \tag{4}$$

Here, G_e is the equilibrium modulus.

The nearly flat frequency response of fluorotelomer grease in the elastic region implies a continuous relaxation time spectrum with $H \approx 1.42$ kPa and $G_e \approx 8$ kPa to provide the smooth curves in Figure 1. Thus, G(t) is derived from the dynamic shear moduli, and plotted in Figure 2 using eq. (3). The shear viscosity from eq. (4) is approximately 45 kPa s. The linear viscoelastic model, with H constant for greases in the elastic region, is not an accurate statement, because it predicts that the grease will eventually flow, given a long enough time under a stress below the yield stress.

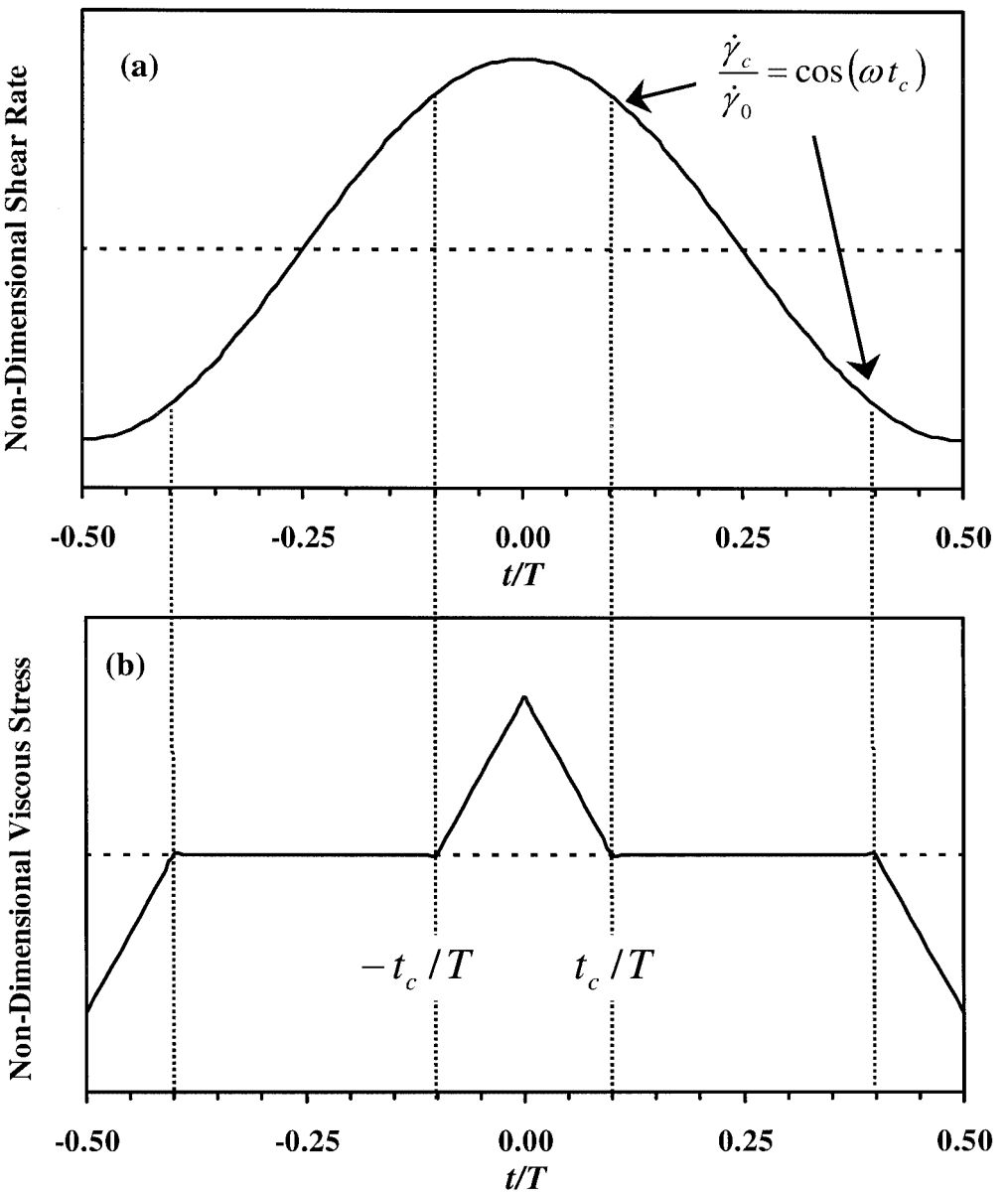

Figure 6 Characteristic features of the viscous slip model showing the relationship between (a) the shear rate and (b) the viscous stress.

Thus, it is likely that outside the time scale which is accessible for measurement with the rheometer, $H \rightarrow \infty$ as $\tau \rightarrow \infty$.

Yield stress

As the shear stress gradually increases, a stress exists at which the viscometer cone fixture gradually begins to rotate. A typical yield stress measurement plot is shown in Figure 3. Initially, the shear rate was below the detection limit of the rheometer, as can be seen by the level of the noise fluctuations. At the yield stress, the viscosity suddenly changed to 2.1 kPa s. The yield stress was determined from such plots by the intersection of the two lines.

For a grease to be useful in bearings, the yield stress must persist throughout the operating temperature range. Yield stress is shown as a function of temperature for three types of grease in Figure 4. All three greases maintain their yield stress to well over 80°C. The yield stress of the gel-thickened lithium grease and the polyurea grease decreased more with temperature than that of the fluorotelomer-thickened grease. The yield stress of the lithium grease in Figure 4 at 20°C is higher than that of the lithium grease shown in Figure 3 because the grease reported in Figure 3 was diluted by 36% with a low viscosity oil.

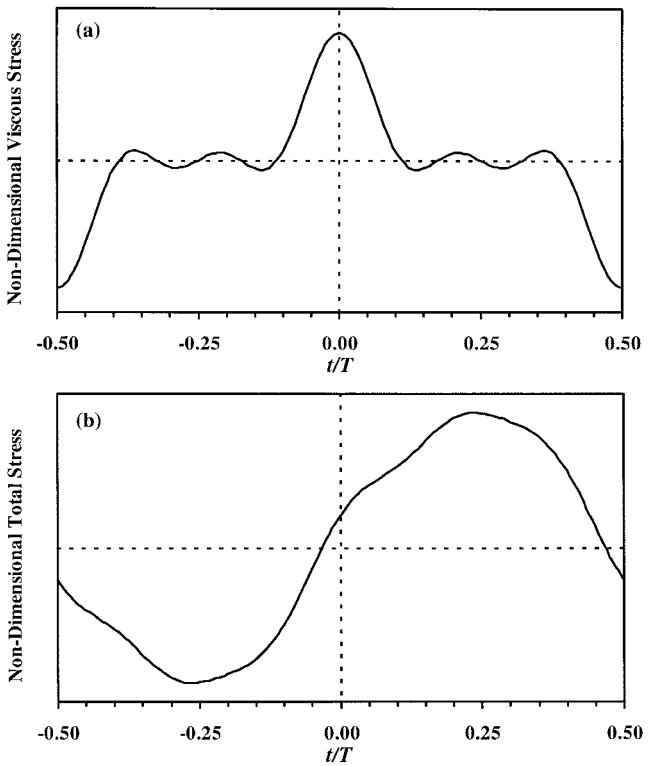

Figure 7 The three-term Fourier series approximation to (a) the viscous stress wave form and (b) the total shear stress. The truncated triangle shape of the viscous stress, Fig. 6(b), is replicated reasonably well by the three-term series in (a). The harmonic distortion and asymmetry is apparent in the total stress (b).

Large amplitude oscillations

When materials with a yield stress are subjected to a periodic shear stress or strain that, for some portion of the oscillation cycle, exceeds the yield point, harmonic distortion of the response waveform is observed. Previously, we described this effect for a carbon black filled polyester[9] and a metal particle suspension.[10] A similar effect is observed with grease. The stress waveform as the shear strain amplitude γ_0 is increased through the yield point is shown in Figure 5 for the fluorotelomer thickened grease. Asymmetric harmonic distortion is clearly visible in the waveform. In our previous work,[9,10] we investigated a purely viscous constitutive model to derive fluid parameters from the harmonics of the waveform. The approach was reasonable, but the model waveform was symmetrical. When the yield stress was exceeded in each cycle at some crossover shear rate, the viscosity decreased from its initial high value to a lower viscosity, symmetrically 'clipping' the stress to a lower level one time in each oscillation cycle.

The Fourier amplitudes of the transformed data for all types of yield stress materials examined in this study clearly indicate a series of decreasing odd harmonics in the waveform. The dual-viscosity model adequately reproduced this series but failed to mimic the asymmetrical shape of the waveform. Subsequent investigation revealed that the asymmetric distortion and odd harmonics could be reproduced simply by the summation of a continuous elastic (in-phase) component, and a discontinuous viscous (out-of-phase) component.

The general form of the new viscous slip stress model is:

$$\sigma = \begin{cases} G\gamma & |\dot{\gamma}| < \dot{\gamma}_c \\ G\gamma + \eta\dot{\gamma}_0\psi(t/T, t_c/T, \ldots) & |\dot{\gamma}| > \dot{\gamma}_c \end{cases} \quad (5)$$

where G is an elastic shear modulus, and $\dot{\gamma}_0$ is the shear rate amplitude. The value of $\dot{\gamma}_0$ is equivalent to $\gamma_0\omega$ where ω equals $2\pi f$. The variable f represents the oscillation frequency in s^{-1}, and the oscillation period T is equal to $1/f$. Material function $\psi(t/T, t_c/T, \ldots)$ is a discontinuous function of time in the oscillation cycle. The crossover time, t_c, is defined by $\dot{\gamma}_c = \dot{\gamma}_0\cos(\omega t_c)$. The material function $\psi(t/T = \pm k/2, \ldots) = 1$ for $k = 0, 2, 4, \ldots$ and $\psi(t/T = \pm k/2, \ldots) = -1$ for $k = 1, 3, 5, \ldots$, as shown in Figure 6. Fourier transformation of this stress model is simplified by its symmetry. The symmetry condition for ψ is $\psi(t) = \psi(-t)$, which yields only Fourier cosine series terms, and $\psi(t/T \pm 1/2) = -\psi(t)$, which yields only odd harmonics.

Fourier transformation of eq. (5) with the triangle wave form for ψ provides a Fourier cosine series approximation for the stress waveform:

$$\sigma - G\gamma = \gamma_0\eta\left(\frac{4}{\pi t_c}\right)\left[\sum_{n=1,3,5,\ldots} \frac{1-\cos(n\omega t_c)}{n^2}\right]\cos(n\omega t) \quad (6)$$

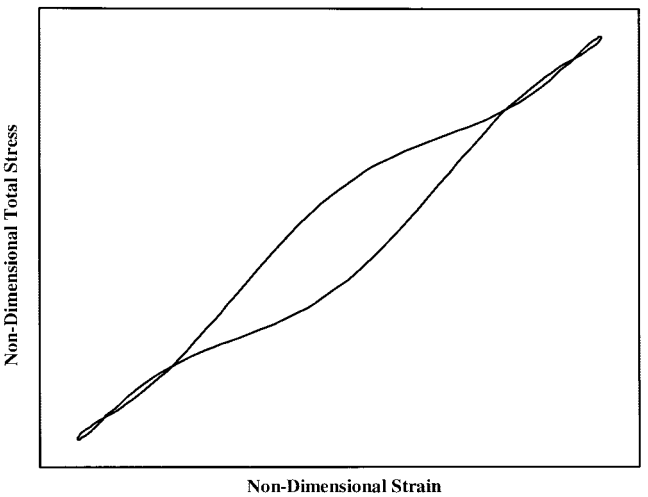

Figure 8 The Lissajous figure corresponding to the wave form in Figure 7.

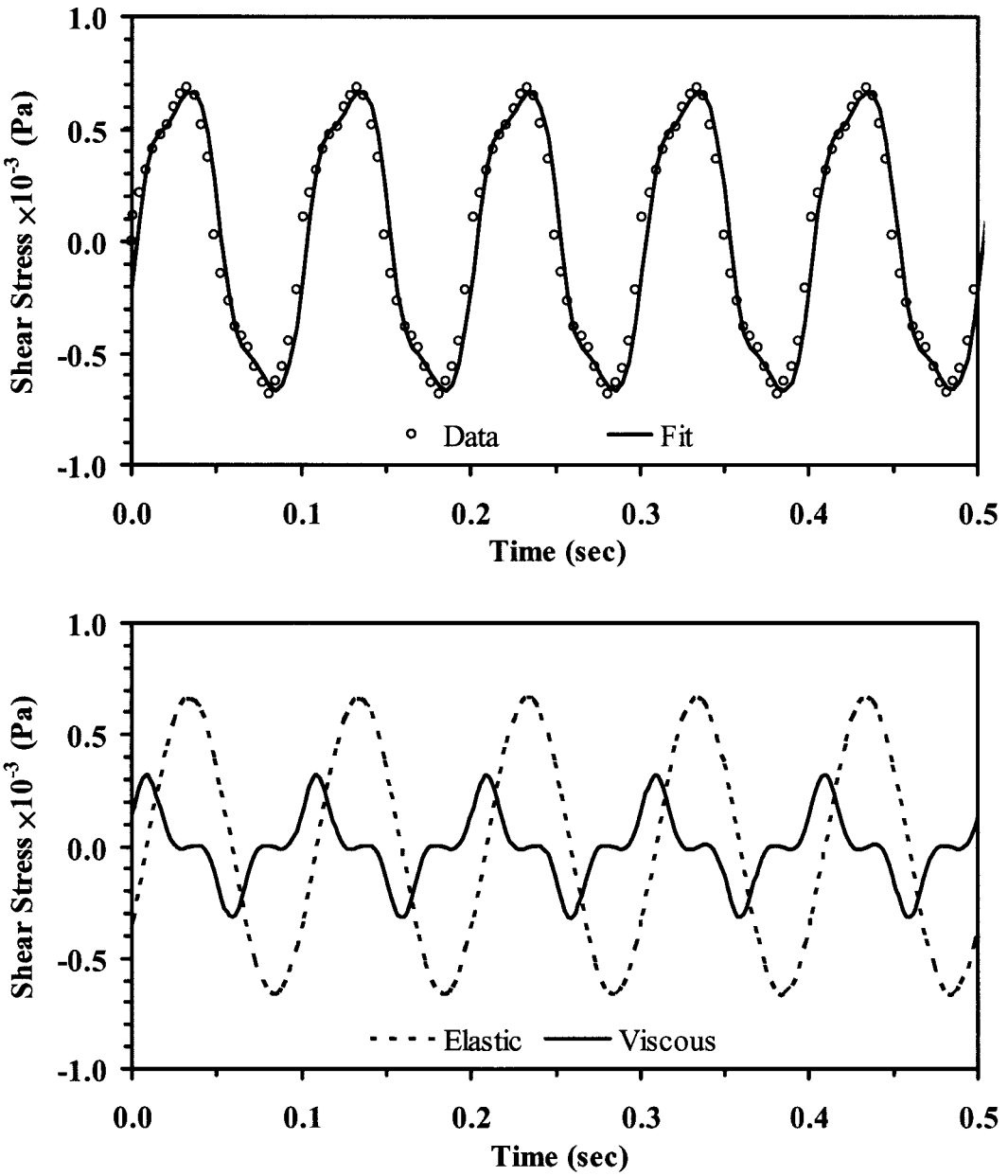

Figure 9 Shear stress wave form comparing the measured stress (open circles) with the fit to Eq. (5), shown by the smooth curve (a). Decomposition of the stress wave into its elastic and viscous parts (b).

Equation (6) contains both the continuous in-phase elastic component $G\gamma$, and the series expansion of the material function, ψ, which is a series of odd harmonics that are proportional to $\gamma_0\eta$ and contain the cross-over time t_c. Since the harmonic amplitudes decrease rapidly with n, the stress waveform is approximately replicated by the first three terms. The three-term approximation of the viscous material function over one oscillation cycle is shown in Figure 7(a), and the total stress waveform is shown in Figure 7(b). A Lissajous Figure, which is commonly employed to detect harmonic distortion, is shown in Figure 8. The shear stress waveform is asymmetric, as reflected in the deviation of the Lissajous figure from its linearly viscoelastic elliptical shape.

The three-term Fourier series expansion of our model, eq. (5), was fit to the numerical LAOS wave form data for several greases. One of these fits is shown in Figure 9. The waveform data is shown by the open circles in Figure 9(a), and the best fit to the model is shown by the smooth curve. Figure 9(b) shows the decomposition of the stress waveform into its continuous elastic and transient viscous stress components. Notice that the viscous component is $\pi/2$ out-of-phase

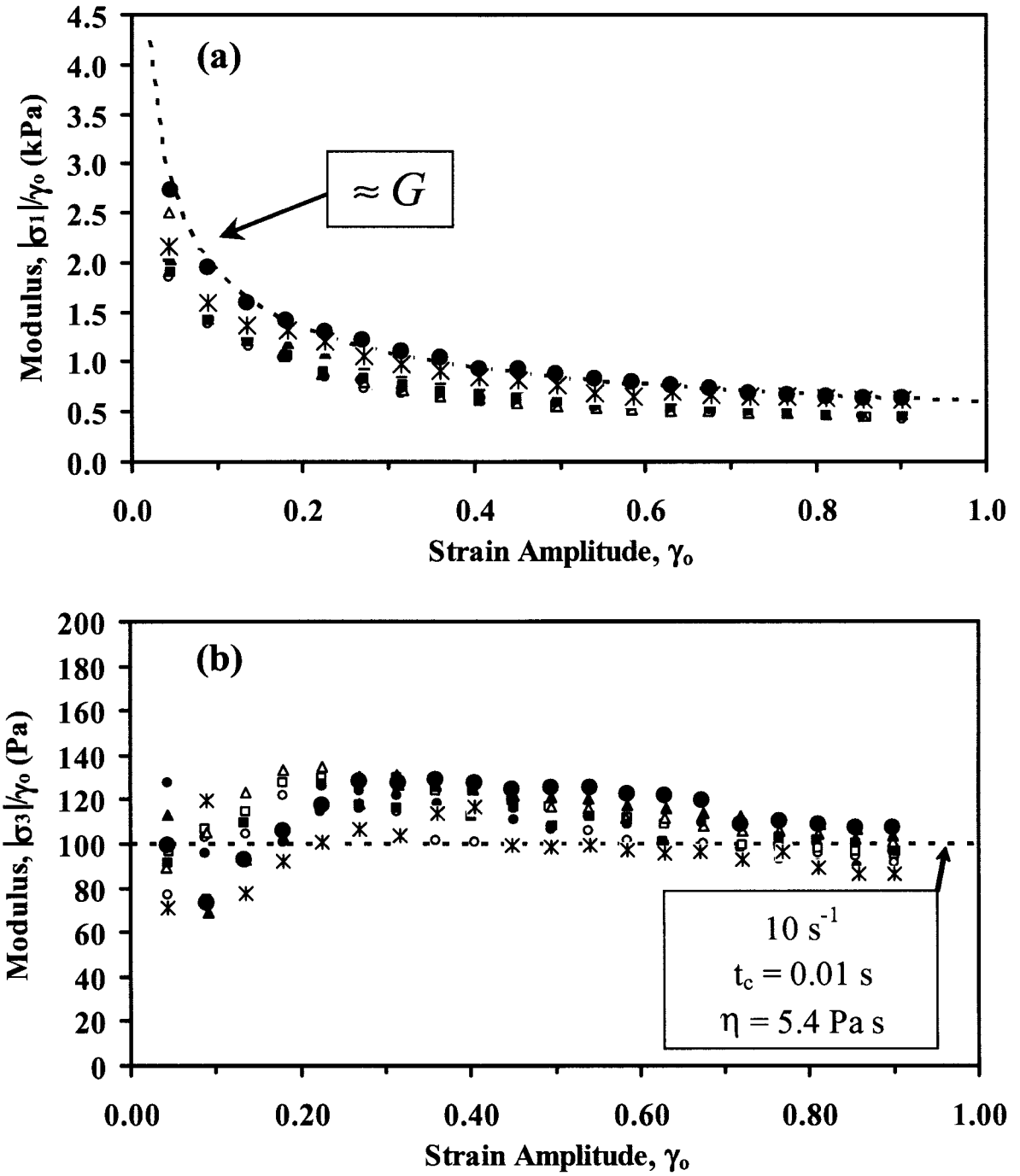

Figure 10 The first harmonic modulus (a), and third harmonic modulus (b), normalized by the strain amplitude of fluorotelomer grease, plotted as a function of strain amplitude, for eight different oscillation frequencies. ○ 0.4 s^{-1}, □ 0.6 s^{-1}, △ 0.8 s^{-1}, • 1 s^{-1}, ■ 2 s^{-1}, ▲ 4 s^{-1}, ∗ 6 s^{-1}, ● 10 s^{-1}.

with the elastic component. The elastic component is proportional to the strain, while the viscous component is activated only when the shear rate exceeds $\dot{\gamma}_c$.

Experimentally, the harmonic amplitudes are the most accessible parametrics of the LAOS waveform. From our model, the stress at the first harmonic ($n = 1$) is:

$$\sigma_1 = \gamma_0 G \sin(\omega t) + \gamma_0 \eta \left(\frac{4}{\pi t_c}\right)(1 - \cos(\omega t_c))\cos(\omega t) \quad (7)$$

Notice that in our approximation, rheometers that calculate G′ and G″ from the phase and magnitude of the first harmonic would report $G' = G$ and $G'' = (4\eta/\pi t_c)[1 - \cos(\omega t_c)]$. The first harmonic modulus ($n = 1$) is then:

$$\frac{|\sigma_1|}{\gamma_0} = \sqrt{G^2 + \left\{\eta\left(\frac{4}{\pi t_c}\right)[1 - \cos(\omega t_c)]\right\}^2} \quad (8)$$

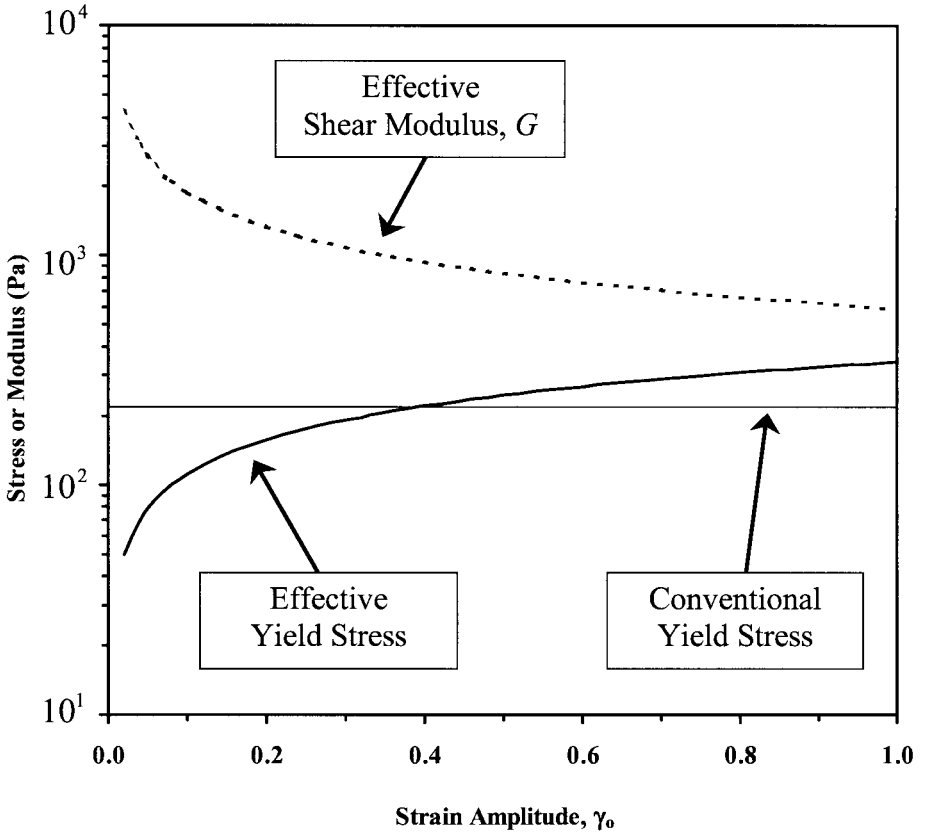

Figure 11 Effective shear modulus and yield stress as a function of shear strain amplitude for the fluorotelomer grease.

The third harmonic modulus ($n = 3$) is:

$$\frac{|\sigma_3|}{\gamma_0} = \eta\left(\frac{4}{\pi t_c}\right)\left[\frac{1 - \cos(3\omega t_c)}{9}\right] \tag{9}$$

The harmonic moduli are compared with measurements on the fluorotelomer thickened grease over a range of strain amplitudes and oscillation frequency in Figure 10. The first harmonic modulus, $|\sigma_1|/\gamma_0$, decreased as ${\gamma_0}^{-1/2}$, which is shown by the dashed curve in Figure 10(a). The harmonic moduli were far less dependent on oscillation frequency than they were on strain amplitude. The third harmonic modulus, $|\sigma_3|/\gamma_0$, had a weak dependence on γ_0, and a slight dependence on oscillation frequency. For this analysis, we set $|\sigma_3|/\gamma_0$ to an average value of 100 Pa, which was consistent with reasonable values of η of 5.4 Pa s and t_c of 0.01 s, shown by the dashed line in Figure 10(b). From this approximation, we find that the first harmonic modulus is dominated by the elastic modulus so that $G \propto {\gamma_0}^{-1/2}$. This probably reflects the increasing breakdown of the microstructure in each oscillation cycle with increasing γ_0. The viscosity never has a chance to recover to its value of 52 kPa s, which was initially measured just above the conventional yield point.

In summary, materials such as grease, which possess a yield stress, appear to respond elastically at low levels of stress or strain, below their yield point. The G′ and G″ are relatively independent of frequency. For example, since $G' \gg G''$ ($G' \approx 10^4$ Pa and $G'' \approx 2 \times 10^3$ Pa) below the yield stress the grease acts like a very lightly crosslinked network.[18] A network of the grease gelling agent, or thickener, consisting of fluorotelomer for PFPE grease, Li 12-hydroxystearate for lithium grease, or polyurea, provides effective crosslinks. When the applied stress exceeds the yield stress, the material begins to flow. Repetitively exceeding the crossover shear rate gives rise to harmonic distortions in the stress wave form at odd multiples of the oscillation frequency. The elastic component is continuous across the yield transition while the viscous, or out of phase, contribution is discontinuous and present only above a certain crossover shear rate. A viscous slip model was adopted for interpretation of the harmonic amplitudes, which accurately fits the actual LAOS waveform. This model provides an effective shear modulus and yield stress, which could be employed in finite element modeling of grease flow in a bearing. The effective yield stress is taken to be the shear stress at the crossover shear rate. Both the effective shear modulus and the effective yield stress are shown in

Figure 11 for the fluorotelomer grease. The effective shear modulus decreases, while the effective yield stress increases, with the shear strain amplitude. The effective yield stress is below the conventional yield stress for $\gamma_0 < 0.4$. These curves reflect the steady state dynamic equilibrium in the kinetics of complex fluid structural network growth and destruction. At low strain amplitude, the network structure dominates the response, presumably influenced by entropic forces. At high strain amplitude, the network is diminished and longer range dissipative motions are observed.

We thank M. Carter and the Hitachi Global Storage Technologies San Jose Materials Analysis Laboratory for some of the stress rheometer measurements, as well as for the use of their stress rheometer throughout the course of measurements performed by R-NK.

References

1. Mas, R.; Magnin, A. J Rheol 1994, 38, 889.
2. Criddle, D. W. Trans Society Rheol 1965, 9, 287.
3. Evans, D.; Hutton, J. F.; Matthews, J. B. J Appl Chem 1952, 2, 252.
4. Binding, D. M.; Hutton, J. F.; Walters, K. Rheol Acta 1976, 15, 540.
5. Bird, R. B.; Dai, G. C. Rev Chem Eng 1983, 1, 1.
6. Wardhaugh, L. T.; Boger, D. V. J Rheol 1991, 35, 1121.
7. Karis, T. E.; Seymour, C. M.; Jhon, M. S. Polym Eng Sci 1991, 31, 99.
8. Carreau, P. J.; De Kee, D. C. R.; Chhabra, R. P. Rheology of Polymeric Systems: Principles and Applications; Hanser Publishers: Cincinnati, OH, 1997.
9. Karis, T. E.; Seymour, C. M.; Kono, R. N.; Jhon, M. S. Rheol Acta 2002, 41, 471.
10. Karis, T. E.; Kim, C. A.; Jhon, M. S. Macromol Mater Eng 2002, 287, 583.
11. Giacomin, A. J.; Dealy, J. M. Rheological Measurement, 2nd Ed.; Collyer, A. A., Clegg, D. W., Eds.; Chapman & Hall: London, UK, 1998.
12. Wilhelm, M.; Maring, D.; Spiess, H. W. Rheol Acta 1998, 37, 399.
13. Yziquel, F.; Carreau, P. J.; Tanguy, P. A. Rheol Acta 1999, 38, 14.
14. Yoshimura, A. S.; Prud'homme, R. K. J Rheol 1988, 32(6), 575.
15. Reimers, M. J.; Dealy, J. M. J Rheol 1998, 42(3), 527.
16. Wihelm, M.; Reinheimer, P.; Ortseifer, M.; Neidhöfer, T.; Spiess, H. W. Rheol Acta 2000, 39, 241.
17. Karis, T. E.; Marchon, B.; Hopper, D. A.; Siemens, R. L. J Fluor Chem 2002, 118(1-2), 81.
18. Ferry, J. D. Viscoelastic Properties of Polymers, 2nd Ed.; John Wiley & Sons, Inc.: New York, 1970, p 43.